Time-Resolved Optical Spectroscopy of Wood

C. D'ANDREA, A. FARINA, D. COMELLI, A. PIFFERI, P. TARONI, G. VALENTINI, R. CUBEDDU, L. ZOIA, M. ORLANDI, and A. KIENLE

CNR-INFM and CNR-IFN, Dipartimento di Fisica, Politecnico di Milano, Piazza Leonardo da Vinci 32, 20133 Milano, Italy (C.D., A.F., D.C., A.P., P.T., G.V., R.C.); Università Milano-Bicocca, Dipartimento di Scienze dell'Ambiente e del Territorio, Piazza della Scienza 1, 20126 Milano, Italy (L.Z., M.O.); and Institut für Lasertechnologien in der Medizin und Meßtechnik, Helmholtzstr.12, D-89081 Ulm, Germany (A.K.)

We have proposed and experimentally demonstrated that picosecond time-resolved optical spectroscopy in the visible/near-infrared (NIR) region (700–1040 nm) is a useful technique for noninvasive characterization of wood. This technique has been demonstrated on both softwood and hardwood samples treated in different ways simulating the aging process suffered by waterlogged woods. In all the cases, alterations of absorption and scattering spectra were observed, revealing changes of chemical and structural composition.

Index Headings: **Time-resolved spectroscopy; Near infrared; Wood; Turbid media.**

INTRODUCTION

Wood is an important material with many applications in everyday life such as in construction, either structurally or nonstructurally, or as fuel.[1] The demand for new wood characterization techniques is always increasing. Beyond industrial applications (e.g., monitoring of the drying process), these techniques have recently been used in the field of heritage conservation to evaluate the state of degradation of wooden objects of artistic, architectural, and archeological interest. In fact, the understanding of the phenomena behind the degradation process is fundamental to designing preservation and consolidation procedures.[2]

Wood is a complex and variable material with structural variations on different scales.[1] According to cellular structure, wood types can be divided into two main classes: softwood (such as spruce, pine, and fir) and hardwood (such as balsa, ash, and chestnut). Softwood presents a simpler structure; in fact, it mainly (about 90%) consists of one type of cells, which are lined up vertically along the tree. The remaining cells are mostly located in bands belonging to the radial plane. Hardwood is composed of four cell types that are orientated in a more complex way, and the total percentage of cells aligned along the vertical axis is between 80% and 95%. It is worth noting, for both softwood and hardwood, that the different distributions of cells along the three axes explain the high degree of anisotropy of wood.

From a chemical point of view, the main constituents of wood are cellulose, hemicellulose, lignin, extractives, and water. Extractives is a collective name for a group of highly complex organic compounds such as lignans, neolignans, and steroids. Lignans and neolignans are aromatic compounds with strong absorption in the ultraviolet (UV)-visible area,[3] and for this reason if they are present in small quantities they contribute strongly to the coloration of the wood. Cellulose is the most abundant polymer in nature and it is formed by a polymerization of glucose. Lignin is the second most abundant polymer in nature. It is amorphous and the structure is formed by random linking of three monolignols.[4] The ratio of these components is dependent on the plant species and morphological origin.[5]

Various techniques are currently used for the study and characterization of wood internal structure. Beyond chemical analysis, the most important techniques are X-rays, solid and liquid nuclear magnetic resonance (NMR), ultrasounds, and microvawes.[6] Each technique allows one to study wood structures with different dimensions and, therefore, each is more suitable according to the specific application and characteristics of the wood sample.

Promising techniques have been developed based on optical radiation. For example near-infrared spectroscopy (NIRS)[7] is employed for the study of pulverized samples extracted from wooden materials because principal absorption lines of the main constituents of wood are located in that spectral range (>1 μm). Recently an optical technique, called GASMAS, was proposed by Andersson et al.[8] for the monitoring of water vapor in wood during the drying process.

Optical radiation has the advantage of being nondestructive, noninvasive, not dangerous for the operators, and relatively simple with respect to many other techniques. In particular, the last point opens the way to the realization of compact and portable instruments to be used in field applications.

The main goal of optical techniques is to separately measure absorption and scattering spectra, which can be related to chemical composition and structure of the sample, respectively. However, discrimination of absorption from the scattering contribution is quite complicated to realize directly on a wood sample due to the nature of wood, which is a highly scattering medium in the visible and near-infrared region. In fact, injected photons undergo many scattering events before being absorbed by or exiting from the sample. Therefore, a simple attenuation measurement does not allow one to discriminate absorption from scattering contributions.

In the last decades a new field of study, called photon migration, has emerged to characterize highly scattering media. These studies have been mainly conducted in the biomedical field,[9,10] although interesting applications have been found in other fields such as the characterization of materials, including plastics, pharmaceuticals, and foods.[11] Different experimental techniques have been developed to study highly scattering media. All of them share the basic scheme of injecting light in one point of the sample and extracting information about it by measuring the properties of the light re-emitted at one or more points on the sample boundary. In this paper we focus on the time-resolved diffuse optical spectroscopy technique, which has given good results in the biomedical field.[12,13] It is worth mentioning that a time-resolved approach, on the nanosecond

Received 6 September 2007; accepted 11 February 2008.
* Author to whom correspondence should be sent. E-mail: cosimo.dandrea@mail.polimi.it.

0003-7028/08/6205-0569$2.00/0

scale, has been proposed to estimate the substantial optical path length in the wood sample.[14]

In this work we propose and experimentally demonstrate that time-resolved optical spectroscopy (TRS), on a picosecond scale, is a valuable technique to characterize wood. In particular, it allows absorption and scattering spectra to be separately obtained by a nondestructive measurement of the sample. It is important to stress that TRS cannot be considered as a surface technique, but is rather a bulk technique. In fact, the typical penetration depth of the technique is from several mm to a few cm, depending on the optical properties of the sample and the distance between the injection and detection points. This work has been mainly motivated to study the degradation state of waterlogged objects of artistic interest. Hence, TRS has been tested on two wood samples (as examples of softwood and hardwood) treated in different ways to simulate the aging process suffered by wet woods.

MATERIALS AND METHODS

Experimental Setup. In the following, the experimental setup for time-resolved optical spectroscopy is briefly described. A detailed description of the system can be found in Pifferi et al.[15] The setup is based on an actively mode-locked Ti:Sapphire laser operating at a repetition rate of 80 MHz and providing light pulses in the wavelength range 700–1040 nm. Through a 1 mm plastic-glass fiber (AFS1000, Fiberguide, NJ), the light pulse is injected into the sample. Diffusely reflected photons exiting the sample are collected by the same type of optical fiber and coupled to a double microchannel plate photomultiplier (R1564U with S1 photochatode, Hamamatsu, Japan). Time-resolved curves are acquired by a time-correlated single photon counting (TCSPC) PC board (SPC-130, Becker & Hickl, Germany). A small part of the injection light is directed, by a fiber optic, to the photomultiplier for online recording of the instrumental response function (IRF).

The time resolution of the system is given by the full width at half-maximum (FWHM) of the IRF, and it is measured to be less than 180 ps. In order to acquire the full time-resolved reflectance spectrum (from 700 to 1040 nm at step of 5 nm), the acquisition time must be about 10 min.

The whole system is completely automated. In particular, a PC controls the laser tuning and power and adjusts the Lyot filters and cavity length of the laser to automatically optimize the IRF. Finally, a stepper motor controls a gradient neutral density filter to regulate the intensity on the detector and compensate the huge change of intensity detected during the measurement.

Time-Resolved Data Analysis. For each wavelength, the absorption and reduced scattering coefficient (μ_a and μ_s', respectively) are calculated by fitting the time-resolved curve to an analytical solution of the diffusion approximation of the transport equation with the extrapolated boundary conditions of an infinite slab.[16] In order to take into account the finite instrumental response function, mainly due to the width of the light pulse, finite response of the detector, and the optical fiber dispersion, the theoretical curve is previously convoluted with the IRF and normalized to the area of the experimental curve. Points of the time-resolved curve with a number of counts lower than 80% of the peak value on the rising edge and 1% on the tail are not included in the fitting range. The fitting process is based on a standard Levenberg–Marquardt algorithm.[17]

Wood Samples. Two different wood types are considered: Silver fir (Abies alba) and Sweet chestnut (Castanea sativa). Both samples have dimensions of $5 \times 5 \times 8$ cm^3 (x, y, and z directions, respectively), where the z direction is parallel to the wood trunk.

The choice of these two wood species is mainly motivated by the need to have a softwood (Silver fir) and a hardwood (Sweet chestnut). In particular, these two species were well diffused in Italy and have been used in the past to realize wood objects. Finally, these woods were supplied by Trees and Timber Institute (IVALSA), which certified the type of wood and the reproducibility of analysis using two different kinds of wood.

For each wood type, three samples were prepared: dry, wet, and degraded. Dry wood is the sample before the treatment. In order to simulate water impregnation, wood was immersed in one liter of bi-distilled water within a hermetically closed box. Then, it remained in an oven at 40 °C for 8 weeks (with weekly change of water). During the first five hours, a reduced pressure was set in order to facilitate the impregnation. A weekly control of weight was performed to evaluate water uptake. In the following, the samples treated with this protocol are called wet woods. Finally a degradation procedure was carried out on the wet sample to simulate the aging process. The wet sample was immersed in a solution of soda (0.1 M) with simultaneous ozone insuflation one hour per day for a period of five weeks and weekly change of soda solution. Finally, the wood sample was washed with bi-distilled water until a neutral pH was obtained. In the following, samples treated with this protocol are called degraded woods. The choice of this degradation procedure was primarily driven by its capability to degrade not only the wood surface but also the wood bulk, at least 2 or 3 cm under the surface. It is worth mentioning that this technique is applied for industrial wastewater treatments in order to degrade recalcitrant compounds such as long chain alkanes.

Measurement Protocol. All the measurements have been carried out by placing the injection and detection optical fibers on the same side of the sample (reflectance geometry). In order to minimize the boundary effects, the measurement is performed in the center of the sample side. Finally, in order to take into consideration the high degree of anisotropy of the wood, each sample is measured with two different orientations of the optical fibers. In the first case, the line connecting the tips of the optical fibers is oriented parallel (par) to the wood z direction, while in the second case, it is perpendicular (per).

It is worth mentioning that the signal intensity showed huge differences according to wood type, treatment, and measurement geometry. Hence, preliminary measurements were performed to define, for each sample, the maximum distance (ρ) between the injection and detection point that gave a satisfactory signal-to-noise ratio to allow the convergence of the fitting algorithm. The choice of the maximum distance, compatible with the signal intensity, is motivated by two facts. First the signal is composed of a higher number of photons that go deep into the sample, and second, the fitting process takes advantage of the larger time span of the signal exiting the sample. In particular, fiber distance varies from 5 mm in the case of dry Sweet chestnut with per geometry, to 25 mm in the case of wet/degraded Silver fir with par geometry.

RESULTS AND DISCUSSION

Dry Wood. In this section we deal with the measurements performed on dry woods. Figure 1 shows absorption and

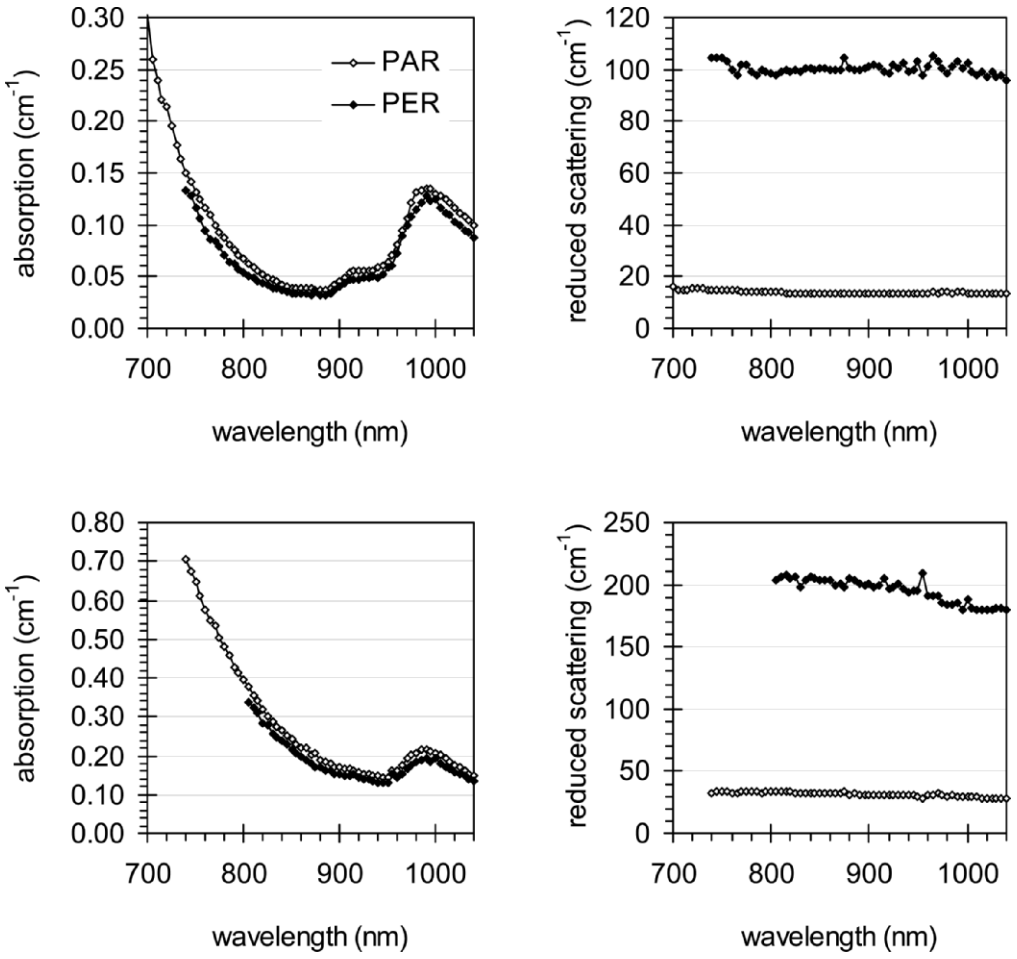

FIG. 1. (**Left**) Absorption and (**right**) scattering spectra of (**top**) dry Silver fir and (**bottom**) dry Sweet chestnut wood along the parallel (open diamonds) and perpendicular (solid diamonds) direction.

scattering spectra of both Silver fir and Sweet chestnut samples for both geometrical configurations (par and per).

Concerning absorption spectra of both wood types, they are overlapped for both geometrical configurations. This indicates that the absorption spectrum is independent of the orientation of the optical fibers with respect to wood structures. This feature is in agreement with the results obtained by Kienle et al.[18] that demonstrated that in a high anisotropy medium the absorption coefficient, as measured in time-resolved reflectance, is independent of the orientation of the injection/detection line.

The absorption spectrum of both types of wood is characterized by a high peak around 1000 nm. The width of the peak around 1000 nm justifies the presence of another absorber beyond water that has a peak around 970 nm.[19,20] This is likely to be attributed to cellulose, as confirmed by preliminary measurements carried out on powder extracted cellulose. Moreover, we observe a rapid increase below 860 nm (for Silver fir) and 900 nm (for Sweet chestnut) towards 700 nm. This can be attributed to lignin and extractives. As expected by the darker color of Sweet chestnut with respect to Silver fir, the increase is more evident with Sweet chestnut. Finally, in the case of Silver fir, a small shoulder around 920 nm is present and it can be ascribed to cellulose. In the case of Sweet chestnut, the absorption peak at 920 nm is no longer visible because of the higher absorption of extractives.

The scattering spectra are particularly flat and horizontal with both wood types and geometrical configurations. This is an indication of a very small scattering power, possibly due to the large size of the scattering centers.[21] This result is quite interesting because it allows one to use a single wavelength system to calculate the reduced scattering coefficient.

Due to the anisotropy of wood structure, scattering values strongly depend on the measurement configuration. In particular, the measurements performed with per geometry give higher values of μ_s' with respect to the parallel configuration. Moreover, the values strongly depend on the type of wood. Hereafter, the average range values with standard deviation are reported. Par geometry: 14 ± 0.7 cm^{-1} and 31.5 ± 2 cm^{-1} for Silver fir and Sweet chestnut, respectively; per geometry: 100 ± 2 cm^{-1} and 195 ± 10 cm^{-1} for Silver fir and Sweet chestnut, respectively. Concerning Sweet chestnut, we observe a slight decrease of the reduced scattering coefficient above 900 nm. This can be attributed to the problem of fitting convergence. In fact, it is worth noting that with Sweet chestnut the higher values of both absorption and reduced scattering coefficients cause a strong reduction of the signal, leading to the loss of some points of the spectrum. In fact the signal-to-noise ratio becomes too low and it does not allow the convergence of the fitting algorithm to extract μ_a and μ_s'.

Finally, in order to quantify the reproducibility of the system

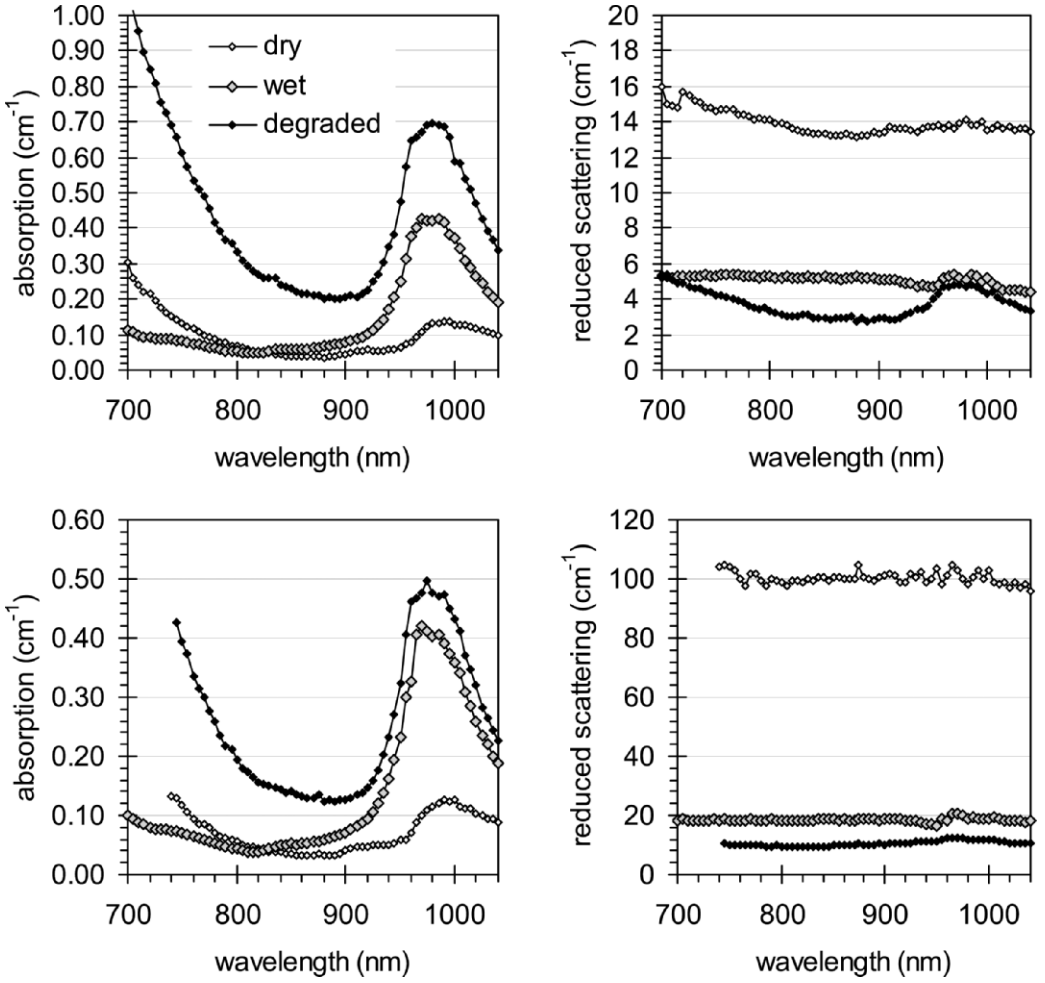

FIG. 2. (**Left**) Absorption and (**right**) scattering spectra of dry (open diamonds), wet (gray diamonds), and degraded (black diamonds) Silver fir along the (**top**) parallel and (**bottom**) perpendicular direction.

results, the same measurements have been repeated on a wood sample (dry fir) on four different days, obtaining a coefficient of variation (CV) of 5.5% and 9.1% for μ_a and μ_s', respectively. Both values are in agreement with the Medphot calibration, which is a common protocol for the performance assessment of diffuse optical spectroscopy instruments.[22] The same homogeneous phantom made of epoxy resin, with TiO_2 powder as the scatterer and black toner as the absorber, has been measured under the same experimental conditions on four different days, obtaining a CV of 5.6% and 6.5% for μ_a and μ_s', respectively. Higher values for the CV of μ_s' in the case of the wood sample can be ascribed to the strong dependence of the scattering coefficient on the re-positioning of the injection/detection fibers with respect to the wood fibers.

Wet Wood. Following the protocol previously described, all the samples were immersed in water. Absorption and scattering spectra of wet Silver fir wood are shown in Fig. 2. In the same figure, the spectra of the dry wood shown in Fig. 1 are also reported in order to facilitate the comparison.

As in the previous case with dry wood, the absorption spectra in both configurations (par and per) are similar. The high water content in the wet sample is clearly revealed by an increase in the absorption coefficient on the water maximum absorption peak at 970 nm. This has the effect of hiding the small peak at 920 nm due to cellulose. Moreover, we observe a decrease in μ_a below 800 nm. This is probably due to the release of water-soluble extractives and low molecular weight compounds in water during treatment. Chemical analyses are currently under development to verify this.

By comparing the absorption spectra of dry and wet samples, we estimated the water increase due to water immersion. This was calculated by taking the difference between the absorption value of dry wood, at 970 nm, and the corresponding value for wet wood. Then, the difference was divided by the water absorption coefficient at the same wavelength. A water content increase of 70% was calculated. An independent measurement of water content increase was carried out from the weight of the dry and wet woods. By assuming that the weight changed only because of water, an increase of 67% was estimated, which is in good agreement with the spectroscopic evaluation.

Scattering spectra of wet Silver fir wood maintain a flat behavior even if the values of the reduced scattering coefficient strongly decrease with respect to dry samples, as confirmed with both the par and per configurations. The reduced scattering coefficient is basically correlated with an index mismatch found by photons during migration into the sample. Then, the huge water presence inside the wood fibers reduces the refractive index mismatch between the interior and exterior part of the fiber, leading to a decrease of the reduced scattering coefficient. In the par configuration, μ_s' decreases to about 5.1

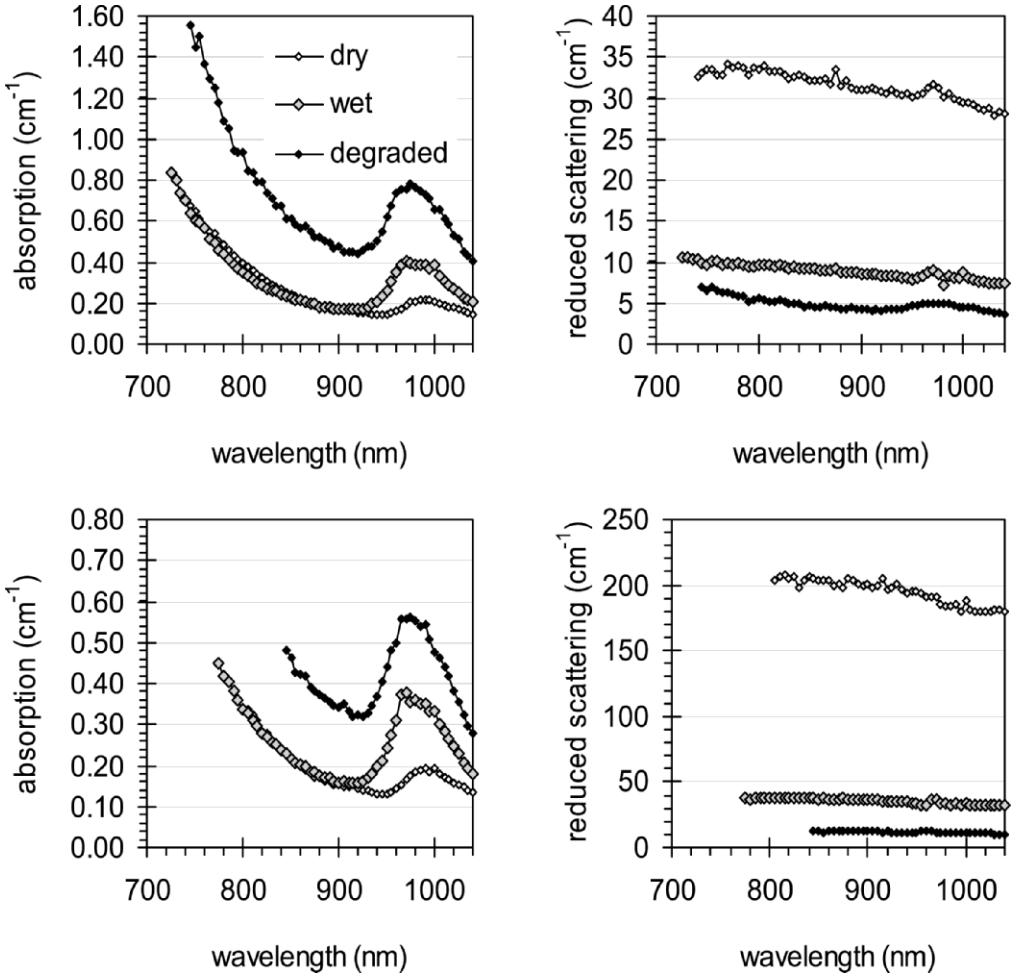

FIG. 3. (**Left**) Absorption and (**right**) scattering spectra of dry (open diamonds), wet (gray diamonds), and degraded (black diamonds) Sweet chestnut along the (**top**) parallel and (**bottom**) perpendicular direction.

$\pm$ 0.3 cm^{-1}, while in the per configuration μ_s' reduces to about 18.5 $\pm$ 0.6 cm^{-1}. Hence, scattering decrease is more evident with per geometry (factor 5.4) rather than with par geometry (factor 2.7). This different behavior between par and per geometry is strongly correlated with the anisotropy behavior of wood. Further measurements and simulations are currently under development to better understand the effect of anisotropy on the quantification of the reduced scattering coefficient.

Absorption and scattering spectra for wet Sweet chestnut wood are reported in Fig. 3. Analogous results to those on Silver fir are clearly visible even though different values for both μ_a and μ_s' are obtained. Concerning absorption spectra, the increase of absorption at 970 nm is evident, while the decrease at 800 nm, even thought few points are available, is not observed. The increase of water content has been calculated from the absorption spectrum, as previously described, obtaining a value of 47%, which is in good agreement with the value of 50% achieved by weight measurements.

Concerning the scattering spectrum, μ_s' reduces by a factor 5.5 and 3.5 in the per and par configurations, respectively. It is interesting to note that these values are similar to the ones previously obtained with Silver fir wood. This seems to indicate that, between dry and wet samples, anisotropy behavior changes in a similar way with the two types of woods.

Degraded Wood. In this section we deal with measurements carried out on samples treated with the artificial aging protocol. In Fig. 2 the absorption and scattering spectra for degraded Silver fir wood are also reported.

Concerning the absorption spectrum, a huge increase below 850 nm is present. This is probably due to oxidation products caused by ozone treatment during the aging process. This is confirmed by the brown color of the wood following the treatment and the presence of an absorption spectrum of the released water where wood was immersed.

Concerning the absorption spectra of degraded Silver fir, we observe an increase above 900 nm with the par and per configurations, making reasonable an increase of water content. At the same time, weight measurements of the sample before and after the treatment do not significantly change. A possible explanation is the further modification of the wood structure due to the aging process. In fact, the reduction of the solid part leaves more space for water, causing the increase of the absorption peak around 970 nm while preserving a similar weight. The reduction of the apparent density has been confirmed by independent measurements carried out with a pycnometer, AccuPyc 1330 Micromeritcs, as reported in the literature by Donato et al.[23]

It is worth mentioning that the absorption spectra measured with the par and per configurations are different, and in particular they are higher with par geometry. This is in contrast

to the results previously obtained with dry and wet samples, where the absorption spectrum is independent of the measurement geometry. The increase of the absorption coefficient with par geometry is probably an artifact due to the quite low scattering value, causing an overestimation of μ_a.

Concerning the scattering spectra, with both the par and per configurations, μ_s' values further reduce with degraded wood: about 3.8 ± 0.8 cm^{-1} and 10.5 ± 0.9 cm^{-1} with par and per, respectively. This suggests that a structural modification took place because of the aging treatment. It is important to stress that these values (especially in the par configuration) are quite low. Hence, the photon migration process is no longer properly described within the diffusion regime. This causes problems of cross-talk between the absorption and reduced scattering coefficient in the fitting process. This aspect is confirmed by two points: (1) the scattering spectrum is less dependent on the absorption line shape with the per configuration rather than the par configuration; and (2) the absorption spectrum in the par and per configurations is different, as previously described, and the second one gives more reasonable values.

Concerning Sweet chestnut (Fig. 3), the results are similar to Silver fir for both the absorption and the scattering spectra. In particular, with the par configuration, the absorption coefficient is higher than with the per configuration. This is mainly due to the effect of cross-talk in the fitting process, as previously described. Moreover, it is also caused by the presence of new absorbing elements that absorb light above 900 nm, as confirmed by the measurement of the absorption spectrum of the released water.

CONCLUSION

In this work we have proposed and experimentally demonstrated that time-resolved optical spectroscopy in the visible/NIR region can be a valuable technique for the nondestructive characterization of wood. The TRS technique has been applied on two types of wood treated in different ways (dry, wet, and degraded). In all the cases, alterations of the absorption and scattering spectra were observed, revealing changes in the chemical and structural composition of the wood. Moreover, the absorption spectra allowed us to estimate the increase in the quantity of water absorbed. To our knowledge, this is the first characterization of wood in the spectral range 700–1040 nm carried out using a time-resolved technique, which, therefore, allows one to discriminate between the absorption and scattering contributions.

Due to the huge variation of wood properties among different species, as well as within the same species, conclusions obtained within a specific application cannot be generalized for all woods and related applications. However, these preliminary results are encouraging, and further study should be carried out on the potential of the time-resolved spectroscopy technique for the optical characterization of wood material at the bulk level.

Further studies will be devoted to correlating the optical parameters with chemical and structural changes measured with other diagnostic techniques (mainly destructive). Moreover, a significant effort will be devoted to the quantification of the wood constituents. This will require the optical characterization of the main constituents of wood, in particular cellulose and lignin. Moreover, improvements of the analysis model will be considered to take into consideration the anisotropy behavior of wood.

As previously stated, this work has been mainly motivated by the study of the degradation of wooden objects of artistic interest. Thus, measurements will be performed for the quantification of the degradation of waterlogged wood objects of archeological and artistic interest and for the monitoring of impregnation and polymerization treatments during the consolidation stage.

In conclusion, we believe that this nondestructive technique can have important applications for the characterization of wooden material because of its simplicity, which can lead to the development of compact and portable systems to be used in the field.

ACKNOWLEDGMENT

This work was partially supported by MIUR under the project PRIN2005 (prot. 2005034194).

1. J. M. Dinwoodie, *Timber: its nature and behaviour* (Taylor and Francis, London, 2000).
2. M. P. Colombini, M. Orlandi, F. Modugno, E.-L. Tolppa, M. Sardelli, L. Zoia, and C. Crestini, Microchem. J. **85,** 164 (2007).
3. D. C. Ayres and J. D. Loike, *Lignans* (Cambridge University Press, Cambridge, 1990).
4. G. Brunow, L. Kilpelainen, J. Sipila, K. Syriainen, P. Karhunen, H. Setala, and P. Rummako, "Oxidative coupling of phenols and the biosynthesis of lignin in Lignin and lignan biosynthesis", in *Lignin and Lignan Biosynthesis,* N. G. Lewis and S. Sarkanen, Eds. (American Chemical Society, Washington, D.C., 1998), p. 131.
5. D. Fengel and G. Wegener, *Wood-Chemistry, Ultrastructure, Reactions* (De Gruyter, Berlin, 1994).
6. V. Bucur, Meas. Sci. Technol. **14,** R91 (2003).
7. S. S. Kelly, T. G. Rials, R. Snell, L. H. Groom, and A. Sluiter, Wood Sci. Technol. **38,** 257 (2004).
8. M. Andersson, L. Persson, M. Sjöholm, and S. Svanberg, Opt. Exp. **14,** 3641 (2006).
9. A. G. Yodh and B. Chance, Phys. Today **48,** 34 (1995).
10. Biomedical Topical Meetings on CD-ROM (The Optical Society of America, Washington, D.C., 2006).
11. R. Cubeddu, C. D'Andrea, A. Pifferi, P. Taroni, A. Torricelli, G. Valentini, C. Dover, D. Johnson, M. Ruiz-Altisent, and C. Valero, Appl. Opt. **40,** 538 (2001).
12. D. Grosenick, K. T. Moesta, H. Wabnitz, J. Mucke, C. Stroszczynski, R. Macdonald, P. M. Schlag, and H. Rinneberg, Appl. Opt. **42,** 3170 (2003).
13. A. Torricelli, A. Pifferi, P. Taroni, E. Giambattistelli, and R. Cubeddu, Phys. Med. Biol. **46,** 2227 (2001).
14. S. Tsuchikawa and S. Tsutsumi, Appl. Spectrosc. **56,** 869 (2002).
15. A. Pifferi, A. Torricelli, P. Taroni, D. Comelli, A. Bassi, and R. Cubeddu, Rev. Sci. Instrum. **78,** 053103 (2007).
16. D. Contini, F. Martelli, and G. Zaccanti, Appl. Opt. **36,** 4587 (1997).
17. W. H. Press, S. A. Teukolsky, W. T. Vetterling, and B. P. Flannery, *Numerical Recipes in C: The Art of Scientific Computing* (Cambridge University Press, New York, 1992).
18. A. Kienle, C. Wetzel, A. Bassi, D. Comelli, P. Taroni, and A. Pifferi, J. Biomed. Opt. **12,** 014026_1 (2007).
19. http://omlc.ogi.edu/spectra/water/.
20. M. Ali, A. M. Emsley, H. Herman, and R. J. Heywood, Polymer **42,** 2893 (2001).
21. C. F. Bohren and D. R. Huffmann, *Absorption and Scattering of Light by Small Particles* (John Wiley and Sons, New York, 1983).
22. A. Pifferi, A. Torricelli, A. Bassi, P. Taroni, R. Cubeddu, H. Wabnitz, D. Grosenick, M. Möller, R. Macdonald, J. Swartling, T. Svensson, S. Andersson-Engels, R. L. P. van Veen, H. J. C. M. Sterenborg, J. M. Tualle, H. L. Nghiem, S. Avrillier, M. Whelan, and H. Stamm, Appl. Opt. **44,** 2105 (2005).
23. I. D. Donato and P. Agozzino, Sci. Technol. Cultural Heritage **13,** 71 (2004).